

¹C. B. Duke, A. Paton, R. J. Meyer, L. J. Brillson, A. Kahn, D. Kanani, J. Carelli, J. L. Yeh, C. Margaritondo, and A. D. Katnani, *Phys. Rev. Lett.* **46**, 440 (1981).

²P. Skeath, I. Lindau, C. Y. Su, W. Chye, and W. E. Spicer, *J. Vac. Sci. Technol.* **17**, 511 (1980).

³L. J. Brillson, R. Z. Bachrach, R. S. Bauer, and J. McMennan, *Phys. Rev. Lett.* **42**, 397 (1979).

⁴A. Huijser, J. Van Laar, and T. L. van Rooy, *Surf. Sci.* **102**, 264 (1981).

⁵R. Z. Bachrach and R. S. Bauer, *J. Vac. Sci. Technol.* **16**, 1149 (1979).

⁶J. R. Chelikowsky, S. G. Louie, and M. L. Cohen, *Solid State Commun.* **20**, 641 (1976).

⁷D. J. Chadi and R. Z. Bachrach, *J. Vac. Sci. Technol.* **16**, 1159 (1979).

⁸J. J. Barton, C. A. Swarts, W. A. Goddard, III, and T. C. McGill, *J. Vac. Sci. Technol.* **17**, 164, 869 (1980).

⁹J. R. Chelikowsky, D. J. Chadi, and M. L. Cohen, *Phys. Rev. B* **23**, 4013 (1981).

¹⁰A. Zunger, to be published.

¹¹E. J. Mele and J. D. Joannopoulos, *Phys. Rev. Lett.* **42**, 1094 (1979), and *J. Vac. Sci. Technol.* **16**, 1154 (1979).

¹²J. Ihm, A. Zunger, and M. L. Cohen, *J. Phys. C* **12**, 4409 (1979), and **13**, 3095 (1980).

¹³D. R. Hamann, M. Schlüter, and C. Chiang, *Phys. Rev. Lett.* **43**, 1494 (1979).

¹⁴E. Wigner, *Phys. Rev.* **46**, 1002 (1934).

¹⁵J. Ihm and J. D. Joannopoulos, to be published.

¹⁶D. Vanderbilt, Ph.D thesis, 1981 (unpublished).

¹⁷K. M. Ho, J. Ihm, and J. D. Joannopoulos, unpublished.

¹⁸D. J. Chadi, *Phys. Rev. Lett.* **41**, 1062 (1978).

¹⁹R. J. Meyer, C. B. Duke, A. Paton, A. Kahn, E. So, J. L. Yeh, and P. Mark, *Phys. Rev. B* **19**, 5194 (1979).

Theory of the Open-Orbit Magnetoresistance of Potassium

M. Huberman and A. W. Overhauser

Department of Physics, Purdue University, West Lafayette, Indiana 47907

(Received 1 May 1981)

The discovery of open-orbit magnetoresistance peaks in potassium shows that its Fermi surface is multiply connected. A charge-density-wave structure (which would have 24 domain orientations and five open-orbit directions per domain) explains the main features. The magnetic field at which open-orbit peaks appear depends on domain size, which we find to be ~ 0.1 mm.

PACS numbers: 72.15.Gd, 72.10.Bg

Recently Coulter and Datars¹ discovered open-orbit magnetoresistance peaks in potassium. Their data on two crystals, obtained with the induced-torque method, are reproduced in Fig. 1. In this paper we show that a charge-density-wave (CDW) structure^{2,3} explains the large number of open-orbit peaks, their field dependence, their width, and variations in the data from run to run.

More than twenty anomalous properties reported during the last eighteen years, which are inconsistent with the prevalent view that potassium has a spherical Fermi surface, have been explained quantitatively or qualitatively by the CDW model. (See Ref. 3 for highlights.) Therefore the authors make no apology for describing as factual the properties of a CDW derived from extensive theoretical and experimental research. Nevertheless, any reader who feels that the data shown in Fig. 1 (which are but two examples of approximately 100 runs on twelve specimens¹) can be reconciled with a horizontal line (demanded by a spherical Fermi surface) is free to substitute the subjunctive mood in what follows.

The CDW wave vector \vec{Q} in potassium has a magnitude⁴ $Q \approx 1.33(2\pi/a)$, 8% larger than the Fermi-surface diameter. Its direction is near a [110] axis⁵ but, because of elastic anisotropy, \vec{Q} is tilted 4.1° away and lies in a plane oriented 65.4° from the cubic (001) plane.⁶ Accordingly there are 24 symmetry-related, preferred axes for \vec{Q} ; so any single crystal will likely be divided into \vec{Q} domains, each having its \vec{Q} along one of these 24 axes. The resulting domain structure, which depends on metallurgical history, is responsible for the nonreproducibility of conductivity data from one run to the next, if the temperature has suffered a large excursion.³

The open orbits are created by three pairs of energy gaps, shown in relation to the Fermi surface in Fig. 2. The main gaps, associated with the CDW periodic potential, cause the 0.6-eV Mayer-El Naby optical anomaly⁴ and distort the Fermi surface nearby to form small necks or points of critical contact. The heterodyne gaps,⁷ shown in Fig. 2, arise from a sinusoidal displacement of the positive ions. The wave vector

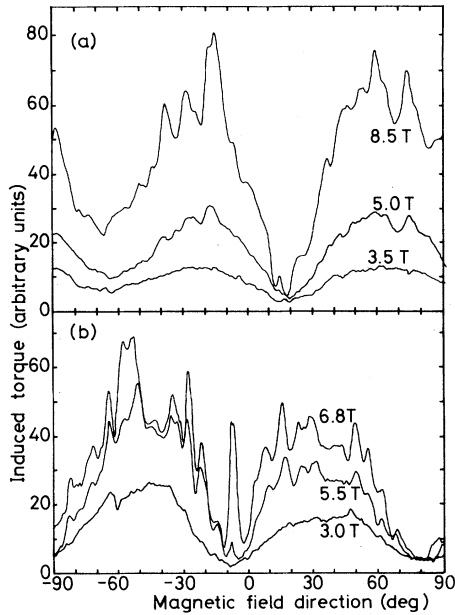


FIG. 1. Magnetoresistance of potassium vs \vec{H} (Coulter and Datars, Ref. 1). (a) Single crystal grown in oil, \vec{H} in a (211) plane. (b) Single crystal grown in a Kel-F mold, \vec{H} in a (321) plane.

$\vec{Q} - \vec{G}_{110}$ of this static displacement lies within the Brillouin zone, unlike \vec{Q} which is much larger. Finally, a third pair of energy gaps arises from a phason instability,⁹ and they are also shown. Other periodicities occur, but we believe their energy gaps to be negligible.

Five open-orbit directions can be identified in Fig. 2. For example, if there is no magnetic breakdown,⁹ an electron traveling in k space on a cyclotron orbit from B to C will be Bragg reflected to D , and will continue to E , where it will be Bragg reflected back to B . The open-orbit direction is $4\vec{Q} - 3\vec{G}_{110}$. However, if the heterodyne gaps at C and D have suffered magnetic breakdown, the electron will travel continuously from B to E , where it will be reflected back to B . The open-orbit direction is then $3\vec{Q} - 2\vec{G}_{110}$. A nonequatorial open-orbit such as G to H (with reflection back to G) can occur even though the same heterodyne gaps have undergone magnetic breakdown on the equatorial orbit at C and D .

It is well known¹⁰ that if a metal has only closed orbits, there can be no high-field magnetoresistance. A nonsaturating magnetoresistance, proportional to \vec{H}^2 , can occur whenever \vec{H} is perpendicular to an open-orbit direction. This effect disappears if \vec{H} is rotated slightly into a nonperpendicular orientation. Sharp magnetoresistance

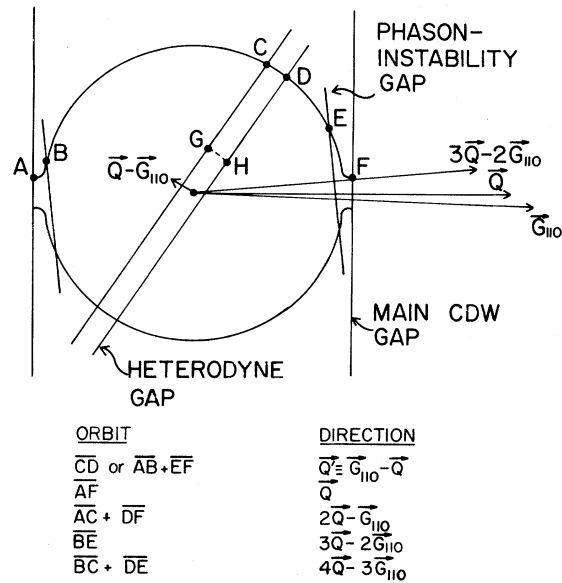


FIG. 2. Fermi surface, energy gaps, and open orbits (for \vec{H} perpendicular to the plane shown).

peaks, observed by rotating \vec{H} (or the crystal), are the signature of open orbits. They provide the method for measuring open-orbit directions. The induced-torque technique,¹ requiring no electrical contacts, has been so utilized for more than a decade.

Obviously a theory for the angular dependence of the magnetoresistivity of a single crystal containing $24 \vec{Q}$ domains, having therefore 120 open-orbit directions, must employ simplifying approximations. We model the magnetoconductivity of a single domain as if it were caused by six Fermi-surface fractions—the dominant one a spherical surface containing $1 - 5 \eta \approx 90\%$ of the conduction electrons. The other five are cylindrical surfaces, each having an axis parallel to one of the open-orbit directions shown in Fig. 2 and containing $\eta \approx 2\%$ of the electrons. The conductivity of a macroscopic single crystal (but broken up into $24 \vec{Q}$ -domain varieties) is calculated by means of the effective-medium approximation.^{11, 12}

Accordingly the conductivity tensor for each type, n , of \vec{Q} domain is given by

$$\vec{\sigma}_n = (1 - 5\eta)\vec{\sigma}_s + \eta \sum_{j=1}^5 \vec{\sigma}_{cnj}. \quad (1)$$

$\vec{\sigma}_s$ is the magnetoconductivity tensor of a spherical Fermi surface and $\vec{\sigma}_{cnj}$ is the magnetoconductivity tensor of a cylindrical Fermi surface having an axis parallel to the j th open-orbit di-

rection of \vec{Q} domain n .¹³ The effective conductivity tensor of the heterogeneous medium is

$$\vec{\sigma}_{\text{eff}} = \vec{\sigma}_{\text{ext}} + \sum_{n=1}^{24} f_n (\vec{\sigma}_n - \vec{\sigma}_{\text{ext}}) \cdot \vec{\beta}_n, \quad (2)$$

where f_n is the volume fraction of \vec{Q} domain n , and $\vec{\beta}_n$ is an explicit tensor, depending on $\vec{\sigma}_n$ and $\vec{\sigma}_{\text{ext}}$, which we have evaluated.¹³ The effective-medium approximation is obtained by requiring the conductivity $\vec{\sigma}_{\text{ext}}$ of the "host," surrounding each domain, to be just $\vec{\sigma}_{\text{eff}}$. This self-consistent tensor,

$$\vec{\sigma}_{\text{eff}} = \vec{\sigma}_{\text{ext}}, \quad (3)$$

can be found quickly by iteration of Eq. (2).

We took the \vec{Q} -domain distribution to be either random ($f_n = \frac{1}{24}$) or textured:

$$f_n = \frac{1}{24} \left[1 + \alpha \left[\frac{3}{2} (\hat{Q} \cdot \hat{T})^2 - \frac{1}{2} \right] \right], \quad (4)$$

where \hat{T} is the unit vector of a texture axis. Finally, the electron scattering time τ for the spherical Fermi surface was taken to be 1.5×10^{-10} sec, appropriate to potassium at 4 °K if the residual-resistivity ratio is ~ 4000 . Then $H = 2$ T corresponds to $\omega_c \tau = 50$.

Since an open orbit is destroyed when it crosses a domain boundary, the relaxation time τ_{open} used in calculating $\vec{\sigma}_{c_n j}$ is shorter than τ , and is given

approximately by

$$\frac{1}{\tau_{\text{open}}} = \frac{1}{\tau} + \frac{8v_F}{3D}. \quad (5)$$

v_F is the Fermi velocity and D is the diameter of a \vec{Q} domain.

The magnetoresistivity ρ_{xx} for \vec{H} in a plane perpendicular to a [211] or a [321] axis was calculated according to the above theory and is shown in Fig. 3. Induced-torque curves were also calculated¹⁴ and, except for the vertical scale, were found to be indistinguishable from the magnetoresistance curves shown. The magnetic field strength at which open-orbit peaks emerge depends somewhat on domain size; $D = 0.05$ and 0.12 mm, respectively, in Figs. 3(a) and 3(b). A texture parameter $\alpha = -1$, with an axis at $\theta = 0$, was used in Fig. 3(a); random orientation, $\alpha = 0$, was used in Fig. 3(b).

The remarkable similarity between Fig. 3 and the data of Fig. 1 illustrates the ease with which (otherwise) incomprehensible data can be explained once one recognizes the CDW structure of potassium. de Haas-van Alphen data, which are sensitive only to closed orbits, can no longer be cited as evidence for a spherical Fermi surface. For then, the only allowed behavior of a magnetoresistance spectrum is the horizontal, dashed line shown in Fig. 3(b).

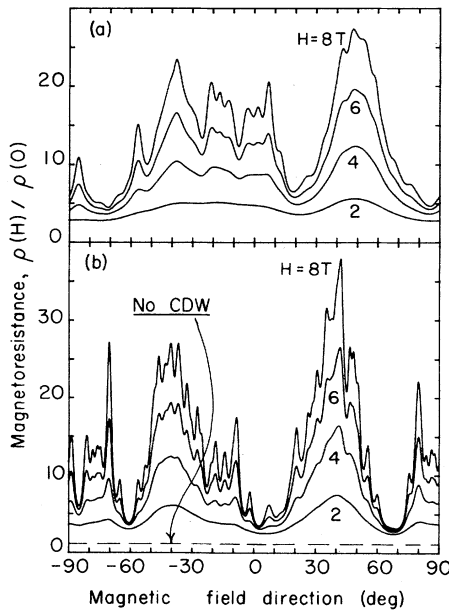


FIG. 3. Theoretical magnetoresistance vs \vec{H} . (a) \vec{H} in (211) plane, $D = 0.05$ mm; texture: $\alpha = -1, \theta = 0$. (b) \vec{H} in (321) plane, $D = 0.12$ mm; no texture ($\alpha = 0$).

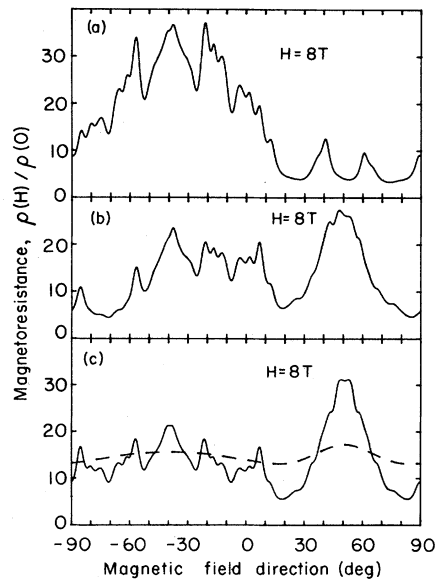


FIG. 4. Theoretical magnetoresistance for \vec{H} in a (211) plane, $D = 0.05$ mm. (a) $\alpha = 2, \theta = 60^\circ$; (b) $\alpha = -1, \theta = 0$; (c) $\alpha = 0$. The dashed curve is for $D = 0.005$ mm.

Until \vec{Q} -domain structure can be experimentally controlled, it will not be possible to make detailed comparisons between theory and data. We illustrate this in Fig. 4, where three spectra are shown for \vec{H} in a (211) plane. Only the texture parameters have been changed. Finally, the dashed curve in Fig. 4(c) shows how open-orbit spectra can be suppressed if metallurgical preparation has caused too small a domain size.

¹P. G. Coulter and W. R. Datars, Phys. Rev. Lett. **45**, 1021 (1980), and private communication.

²A. W. Overhauser, Phys. Rev. **167**, 691 (1968).

³For an experimental and theoretical review, see A. W. Overhauser, Adv. Phys. **27**, 343 (1978).

⁴A. W. Overhauser, Phys. Rev. Lett. **13**, 190 (1964); A. W. Overhauser and N. R. Butler, Phys. Rev. B **14**,

3371 (1976).

⁵A. W. Overhauser, Phys. Rev. B **3**, 3173 (1971).

⁶G. F. Giuliani and A. W. Overhauser, Phys. Rev. B **20**, 1328 (1979).

⁷J. R. Reitz and A. W. Overhauser, Phys. Rev. **171**, 749 (1968).

⁸G. F. Giuliani and A. W. Overhauser, Bull. Am. Phys. Soc. **26**, 471 (1981).

⁹E. I. Blount, Phys. Rev. **126**, 1636 (1962).

¹⁰I. M. Lifshitz, M. Ia. Azbel, and M. I. Kaganov, Zh. Eksp. Teor. Fiz. **31**, 63 (1956) [Sov. Phys. JETP **4**, 41 (1957)].

¹¹D. A. G. Bruggeman, Ann. Phys. (Leipzig) **24**, 636 (1935).

¹²R. Landauer, J. Appl. Phys. **23**, 779 (1952); D. Stroud and F. P. Pan, Phys. Rev. B **20**, 455 (1979).

¹³M. Huberman and A. W. Overhauser, Phys. Rev. B **23**, 6294 (1981).

¹⁴P. B. Visscher and L. M. Falicov, Phys. Rev. B **2**, 1518 (1970).

Role of Adsorbed Water in the Dynamics of Metmyoglobin

G. P. Singh,^(a) F. Parak,^(b) S. Hunklinger, and K. Dransfeld

Max-Planck-Institut für Festkörperforschung, D-7000 Stuttgart 80, West Germany
(Received 13 April 1981)

By microwave measurements we have determined the dielectric relaxation rate for adsorbed water in metmyoglobin crystals in the temperature range from 100 to 300 K. The temperature dependence of the dielectric relaxation rate of the adsorbed water is nearly identical to the temperature dependence of the conformational fluctuation rate of the protein as measured by the Mössbauer effect. This surprising correlation may be understood in terms of the mechanical and electrical interactions between the adsorbed water and the protein.

PACS numbers: 77.40.+i, 87.15.-v

The physiological function of proteins cannot be understood from their static structure since dynamical aspects are of great importance. Recently x-ray¹ and Mössbauer²⁻⁴ studies on myoglobin crystals and frozen solutions have revealed that the atoms in the protein molecule undergo unusually large displacements. For example, the average displacement of the Fe atom in myoglobin is as large as 0.24 Å at room temperature. Such anomalously large values can be ascribed to the fluctuations between conformational substates of the protein molecule.¹ These substates arise from a large number of slightly different structural configurations which protein molecules can adopt. In Mössbauer experiments it was found that the characteristic time of these large-amplitude motions is about 10⁻⁷ s at room temperature.⁴ On cooling, however, these fluctuations slow down, and below 200 K, they are too slow to

be seen by Mössbauer experiments.

Mössbauer experiments on proteins^{5,6} and Rayleigh scattering experiments on myoglobin⁷ powders with controlled water content have already shown that the large displacements of the iron atom disappear if the amount of water adsorbed on the protein is reduced. Therefore to understand the role played by water, we have studied the dynamical dielectric properties of water in metmyoglobin crystals. We find that the temperature dependence of the dielectric relaxation rate of the adsorbed water in metmyoglobin crystals is strongly correlated to the temperature dependence of the displacement of the iron atom as seen by Mössbauer measurements. In this paper we discuss how the dynamic dielectric properties of the adsorbed water may influence the conformational fluctuations inside the protein.

Dielectric measurements at microwave frequen-